Revista Mexicana de Ingeniería Química

Ingeniería de alimentos

PREPARATION OF STARCH/CLAY/GLYCEROL NANOCOMPOSITE FILMS AND THEIR FTIR, XRD, SEM AND MECHANICAL CHARACTERIZATIONS

PREPARACIÓN DE PELÍCULAS CON NANOCOMPUESTOS DE ALMIDÓN/ARCILLA/GLICEROL Y SU CARACTERIZACIÓN MECÁNICA, FTIR, XRD Y SEM

M.C. López-Chavez[1], G. Osorio-Revilla[2], S. Arellano-Cárdenas[1], T. Gallardo-Velázquez[1], S.O. Flores-Valle[3], MS. López-Cortez[1]*

[1]*Departamento de Biofísica.* [2]*Departamento de Ingeniería Bioquímica. Escuela Nacional de Ciencias Biológicas-IPN, Prol. de Carpio y Plan de Ayala, s/n. Col. Santo. Tomás. Apartado Postal 42-186, C.P. 11340, Ciudad de México. México.*
[3]*Laboratorio de Catálisis. Escuela Superior de Ingeniería Química e Industrias Extractivas-IPN. Unidad Profesional Adolfo López Mateos. Colonia Lindavista, Gustavo A. Madero, C.P. 07738, Ciudad de México, México.*

Abstract

In the present work, Mexican natural clay (NC) was used to prepare an organoclay (OC), and both were added to a mix of starch/glycerol to obtain nanocomposite films of starch (TPS)/clay/plasticizer. The average thickness of the TPS/5% NC/25% glycerol films was 81± 3 μm, and it was 91± 2 μm for the TPS/5% OC/25% glycerol films. Both the X-ray diffraction and infrared analyses showed that the glycerol and starch molecules can be intercalated into the clay galleries. A good dispersion of the components in the mix was observed via an electron scanning microscope. Using the nanoindentation method, it was observed that the materials with the highest elasticity had the lowest amount of clay and the highest concentration of glycerol. The moisture permeability of the films was reduced by 80% in the presence of the clay materials utilized in this study.

Keywords: clay, composite films, organoclay, thermoplastic starch.

Resumen

En la presente investigación se utilizó una arcilla natural (NC) de origen mexicano a partir de la cual se preparó una organoarcilla (OC). Las arcillas natural y orgánica, se adicionaron a una mezcla de almidón/glicerol para obtener películas con nanocompuestos de almidón (TPS)/arcilla/plastificante. El espesor promedio de las películas preparadas con TPS/5% NC/25% glicerol fue de 81 ± 3 μm, y de 91 ± 2 μm para las películas TPS/5% OC/25% glicerol. Los análisis de difracción de rayos X e infrarrojo mostraron que las moléculas de almidón y de glicerol pueden intercalarse en la región interlaminar de la arcilla. Mediante la microscopía electrónica de barrido se observó una buena dispersión de los componentes en las mezclas. Por el método de nanoindentación, se observó que las películas con mayor elasticidad fueron las que contenían menor cantidad de arcilla y mayor concentración de glicerol. La permeabilidad al vapor de agua de las películas preparadas se redujo en un 80% con la presencia de las arcillas utilizadas.

Palabras clave: arcilla, películas, nanocompuestos, organoarcilla, almidón termoplástico.

1 Introduction

Currently, it is possible to find many studies on the preparation of biodegradable thermoplastic starch (TPS) composite films, which can be used for food packages. Usually, TPS films are obtained via structural modification inside starch granules processed with a low water content under thermal and mechanical forces, and starch may be combined with plasticizers, such as glycerol, which are not easily evaporated during the processing (Avella *et al*., 2004; Villada *et al*., 2008; Borges *et al*., 2015; Esmaeili *et al*., 2017). However, TPS films have low mechanical stability and are sensitive to moisture due to the highly hydrophilic nature of its components. Such properties may be improved by the addition of other materials, such as cellulose fiber, nano-clays or other biodegradable polymers (Park *et al*., 2003; Averous and Boquillon, 2004; Chang *et al*., 2010; Fialho and Moraes *et al*., 2017; Khan *et al*., 2017; Flores-Martínez *et al*., 2017). A promising alternative

* *Corresponding author. E-mail*: socolc@prodigy.net.mx

is the preparation of nanocomposites by combining biopolymer-clays (Azeredo, 2009; Santos *et al.*, 2014; Wilpiszewska *et al.*, 2015; Cheviron *et al.*, 2016; Staroszczyk *et al.*, 2017). Natural clays (NC), such as montmorillonites, have a laminar structure and are readily available, non-toxic and inexpensive. Mexican montmorillonites have suitable properties, such as cation exchange, surface area and swellability, that make them very versatile and readily modifiable via the intercalation of surfactants (typically quaternary ammonium salts) in the interlaminar region to obtain hydrophobic organoclays (OC) (López *et al.*, 2008; Arellano-Cárdenas *et al.*, 2012, 2013; Almazán-Sánchez *et al.*, 2016; Jiménez-Castañeda and Medina, 2017). Recent research has shown that the use of the right combination of starch/NC or OC plus glycerol as a plasticizer may improve the physical properties of films, such as the thermal stability, and decrease their permeability to water vapor and gases, such as O_2 and CO_2 (Park *et al.*, 2003; Yu *et al.*, 2007; Zhang *et al.*, 2007; Kho *et al.*, 2008; Rhim *et al.*, 2009; Cyras *et al.*, 2008; Hongguang *et al.*, 2009; Gao *et al.*, 2014; Chung *et al.*, 2010; Müller *et al.*, 2012, 2014; Romero-Bastida *et al.*, 2015; Nguyen *et al.* 2016;). Nevertheless, the incorporation of-nanoclays onto a TPS matrix to obtain homogeneous films with good mechanical and barrier properties has remained a challenge because the chemical and physical properties depend on the type and origin of the clay and its morphological and chemical characteristics.

The present study proposes the use of a Mexican NC with a hydrophilic nature and the hydrophobic OC obtained from it for the preparation of TPS/clay/glycerol nanocomposite films. The effect of both materials on the microstructure and mechanical and barrier properties of the obtained films is described.

2 Materials and methods

2.1 Materials

The natural clay used in the present work was a Perfobent montmorillonite from northern Mexico and was supplied by Arcillas Industriales de Durango, S.A. This clay was sieved through a number 65 sieve (mesh size 0.210 mm). Preparation and characterization of the OC was described previously by López *et al.*, 2008, and the surfactant cetylpiridinium chloride (CPC) ($C_{21}H_{38}ClN·H_2O$ from Sigma-Aldrich Chemical Co.) was added to the NC in an amount equivalent to 100% of its cationic exchange capacity (CEC). The CEC value reported for the NC is 101 meq/100 g and 45 meq/100 g for the OC. The basal spacing d(001) values for NC and OC are 1.24 and 2.14 nm, respectively.

2.2 Preparation of the films

The starch-based films were prepared according to the methods proposed by Park *et al.*, 2003, and Lilichenco *et al.*, 2008, with some modifications. Clay (NC or OC) was dispersed in water, and starch was gelatinized in hot water at 90°C. Then, both suspensions were mixed to obtain three proportions starch/clay on a dry basis (95/5, 90/10, 85/15) and glycerol was added at two concentrations of 25 and 30%, based on the amount of starch on a dry basis. The mix was stirred and placed in a sonicator (ultrasonicator Branson 1200, Bransonic 50/60 HZ, 117 volts, 0.7 amperes) for 30 min. The films were obtained by casting them in polyethylene Petri dishes 8.5 cm in diameter and drying them at 50 °C for 24 h in a THELCO model 19 vacuum stove. The dried films were peeled off and stored in a vacuum desiccator until further analysis. Three types of films were obtained: pure starch (TPS)/glycerol, TPS/NC/glycerol and TPS/OC/glycerol composite films.

2.3 Characterization of the films

The thickness of the films was determined using a Mitutoyo electronic micrometer (sensitivity of 1 μm) by measuring ten different points along the film (Müller *et al.*, 2012; Sothornvit and Krochta, 2001). The films obtained were read directly in an FTIR Perkin Elmer Spectrum 2000 spectrophotometer using 8 scans and 4000 to 400 cm^{-1} as the wavenumber range (Chang *et al.*, 2010). Diffractograms were recorded for the powders (NC, OC and starch) or films using a Siemens D-500 diffractometer with a nickel filter and Cu Kα radiation of λ = 1.5406 Å, operating at 30 kV and 20 mA and scanning the 2θ angle from 2 to 64°. The basal spacing d(001) was calculated using Bragg's equation (Brindley and Brown, 1980). Images of the microstructures of the films (degree of dispersion) were obtained using an electron scanning microscope, JEOL model JSM-5800 LV.

The mechanical properties were determined according to the method reported by Fisher, 2006. Samples of 1 cm^2 were cut and pasted with glue on a slide. The samples were fixed on a support,

and the moving axis was operated with computer software. The conditions of the test were a maximum load of 5 mN (miliNewtons), a load speed and unloading of 15 mN/min and a pause of 15 s. The instrument used in this study was a Nanoindentator NHT, CSM Instruments (Switzerland), with an optic microscope coupled to a Berkovich diamond tip (standard). The Oliver and Pharr 1992 method was used to calculate the tensile strength (TS) and elastic modulus (Young's modulus, E) via a puncture test. The nanoindentator software draws the graphic strength *versus* the penetration to obtain the punctual S slopes, which allow the calculation of TS and E.

The velocity of the moisture transmission was measured using the Payne Permeability cup, according to ASTM E96-80 and following the technique proposed by Ning *et al.*, 2010 with some modifications. Samples 7 cm in diameter were cut and placed in the base of a cell that contains calcium chloride, $CaCl_2$, as a desiccant, and the samples were secured with a metallic ring and screw cap, leaving an exposed area of 25 cm^2 for the exchange. Additionally, a desiccant with 300 mL of a saturated solution of $Mg(NO_3)_2$ was prepared to give a relative humidity (RH) of 51.4%. This solution was obtained via hot mixing and magnetic stirring 235 g of magnesium nitrate hexahydrate $Mg(NO_3)_2 \cdot 6H_2O$ and 300 mL of distilled water. When the solution was cooled to 30°C, the formation of nitrite salt crystals was observed, which indicated the formation of a saturated solution. To secure the homogeneity of the RH, a fan was coupled under the ceramic base of the desiccator, and foam was placed between the rim and the lid. Once the lid was closed, the system was placed inside a stove at a controlled temperature of 30°C. The capsules were weighed, and the first reading was recorded at time zero. Afterwards, the capsules were placed back into the desiccator, and the weights of the capsules were recorded again at one hour time intervals for seven hours.

The water vapor transmission rate (WVTR) was calculated using a linear regression of the slope of the weight gained in the test cup (G) *versus* the time (t) and dividing the slope by the exposed area of the films (A), as shown in Eq. (1):

$$WVTR = \frac{G}{tA} \qquad (1)$$

Permeance was calculated using Eq. (2):

$$Permeance = \frac{(WVTR)}{P2 - P1} \qquad (2)$$

where P_2 and P_1 are the partial pressures at the inner surface of the films and the surface of the desiccant, respectively. The value of P_1 was considered to be zero, while P_2 was calculated using RH = 51.4% in the desiccator and Psat of 4.24 kPa, which is the pressure of the saturation of water vapor at 30°C.

The water vapor permeability (WVP) was calculated as the product of the permeance and the average thickness of the film.

Each sample was analyzed in triplicate, and the WVP value for each film is presented as the mean and standard deviation of these results.

3 Results and discussion

3.1 Thickness of the films

The determination of the thickness of the films is important because this parameter affects the mechanical and barrier properties. Table 1 shows the thicknesses of the films made with different proportions of TPS/clay/glycerol. The values are the average of three samples, and each one was measured in ten different areas, as explained in the materials and methods section. The thickness of the pure starch and 25% glycerol film registered an average of 85±5 ?m and 53±6 μm for the pure starch and 30% glycerol film. Regarding the TPS/NC films, it was observed that higher proportions of natural clay slightly increased the thickness for both proportions of glycerol. The TPS/OC films (mean thickness value of 89 ±5 μm) showed the glycerol content had no effect on the thickness. When the clay proportion increases, a small increase in the thickness was observed, although this difference was not statistically significant. Regarding the type of clay, it was observed that the TPS/NC films have lower thicknesses (mean values of 81±5 μm for 25% glycerol and 62±5 μm for 30% glycerol) compared to the TPS/OC films (mean thickness value of 89 ±5 μm). The thicknesses obtained for the films using two types of clay are within the values reported for starch/clay biofilms. Souza *et al.*, 2012, reported a range of 76.72 to 91.84 μm, and Borges *et al.*, 2015, reported a range of 60 to 80 μm.

Table 1: Thickness (μm) of TPS/NC and TPS/OC starch/clay composite films with 25% and 30% glycerol content

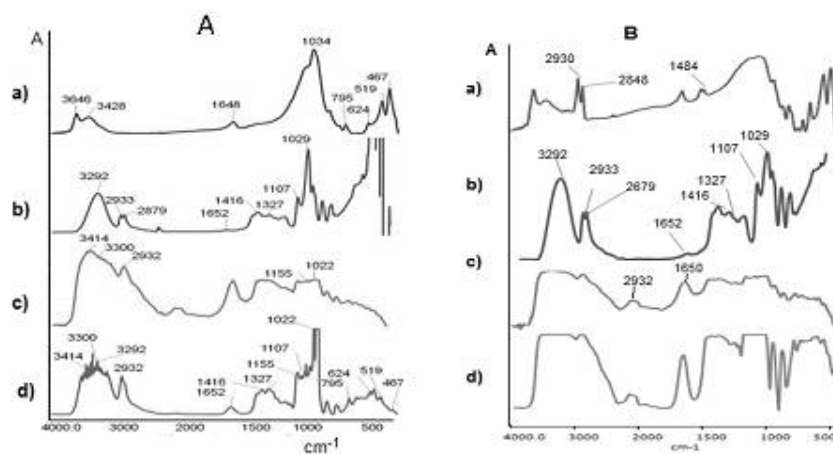| | glycerol | | | glycerol | |
TPS/NC	25%	30%	TPS/OC	25%	30%
100/0	85±5	53±6	–	–	–
95/5	75 ± 2	59 ± 5	95/5	83 ± 5	88 ± 3
90/10	84 ± 5	64 ± 3	90/10	96 ± 2	85 ± 2
85/15	86 ± 3	64 ± 3	85/15	96 ± 8	89 ± 5

Fig. 1 A) FTIR spectra of a) Natural clay, b) glycerol, c) TPS and d) TPS/NC 95/5, 25% glycerol film. B) FTIR spectra of a) Organoclay, b) glycerol, c) TPS and d) TPS/OC 95/5, 25% glycerol film.

3.2 Infrared analysis (FTIR) of the films

Fig. 1A shows the IR spectra for each component of the TPS/NC film with a starch/clay ratio 95/5 and 25% glycerol. Fig. 1A (a) corresponds to the IR spectrum of the NC, whose main bands are at 3646 and 3428 cm^{-1} (OH stretching), 1648 cm^{-1} (OH flexion) and 1034 cm^{-1} (stretching of the Si-O and Si-O- bonds in the structure) (López *et al*., 2008). The IR spectrum of the glycerol molecule, Fig. 1A (b), shows absorption bands at 3292 cm^{-1} (OH groups), 2933 cm^{-1} and 2879 cm^{-1} (stretching of the CH groups for CH_3 and CH_2, respectively), 1652 cm^{-1} (OH groups), 1416 and 1327 cm^{-1} (CH groups), and 1107 and 1029 cm^{-1} (OH groups). Fig. 1A (c) corresponds to the IR spectrum of starch, and a wide band is located between 3300 and 3414 cm^{-1}, which is attributed to the stretching of the OH groups in the glucose molecule. The width of the band indicates the presence of intermolecular hydrogen bonds in the structure of starch, and the peak at 2932 cm^{-1} is due to the stretching vibrations of the CH_2 in the glucose rings. The last bands in this spectrum are at 1155 cm^{-1} (stretching vibrations of C-O in the C-OH groups) and 1022 cm^{-1} (stretching vibrations of C-O in the C-OC groups) (Huang *et al*., 2004, Ruiz, 2006.). The IR spectrum of the TPS/NC film (95/5, 25% glycerol), Fig. 1A (d), shows intense bands due to the thickness of the film (81±2 μm), which agrees with other reports on plastic films of this type (Wilhelm *et al*., 2003). It has also been reported that NC, glycerol and starch may present a physical interaction with hydrogen bonds (Dean *et al*., 2008). The spectrum of the film has a shift in the pure NC band (3428 cm^{-1}) to a lower wavelength (3414 cm^{-1}), which is characteristic of the hydroxyl groups that participate in the formation of hydrogen bonds. Santos *et al*., 2014, suggested that this indicates a possible interaction among starch, glycerol and clay molecules. The peak at 2932 cm^{-1} (in the starch spectrum) did not change; therefore, as mentioned by Majdzadeh *et al*. (2010), the glucose ring does not seem to be involved in the plasticizing process.

Table 2: XRD parameters: 2θ angle and basal spacing d(001) of clay (NC and OC); TPS/NC and TPS/OC starch/clay composite films with 25% and 30% glycerol content.

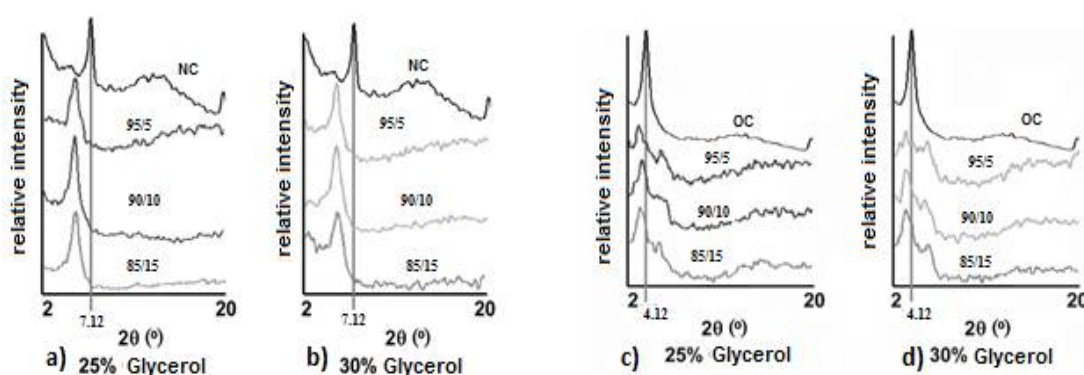| glycerol content (%)	Composition TPS/clay	NC		OC	
		2θ (°)	d(001) (nm)	2θ (°)	d(001) (nm)
	Clay	7.12	1.24	4.12	2.14
	95/5	4.96	1.78	3.24	2.73
25	90/10	5.11	1.73	3.51	2.51
	85/15	5.08	1.74	3.67	2.41
	95/5	4.99	1.77	3.5	2.52
30	90/10	5.01	1.76	3.62	2.44
	85/15	4.84	1.82	3.44	2.56

Fig. 2 XRD diffractograms of natural clay, organoclay and composite films: a) and b) TPS/NC; c) and d) TPS/OC, with proportions TPS/clay 95/5, 90/10, 85/15 with 25% and 30% of glycerol.

The FTIR spectra of the TPS/OC composite films are shown in Fig. 1B and are similar to the ones obtained for the TPS/NC films. The FTIR spectrum of OC in Fig. 1B (a) shows the same bands as the host clay with additional strong bands at 2930 and 2848 cm^{-1} (asymmetric and symmetric stretching vibrations, respectively, of the -CH$_2$ groups in the aliphatic hydrocarbon chains) and a peak at 1484 cm^{-1} (indicative of the -CH$_2$ bending vibration mode). These peaks indicate the presence of the CPC surfactant intercalated in the natural clay (López *et al.*, 2008). In Fig. 1B (d), an overlap of the main bands makes it difficult to distinguish them. A very intense band is observed in the region of 3000 - 3500 cm^{-1}, which is due to the responses from each component in the OH, CH$_2$ and CH$_3$ groups. The similarities in the spectra of the mixes suggest that the interaction between starch and glycerol is physical in nature and not chemical (Ruiz, 2006).

3.3 X-ray diffraction (XRD) of the films

Fig. 2 shows the diffractograms of the TPS/NC and TPS/OC films and compares them to those of pure NC and OC. The characteristic first-order reflection peak d(001), is related to the basal spacing between the silicate sheets. Table 2 summarizes the values for the 2θ angle of the peaks and the corresponding d(001) distances calculated using Bragg's equation (mean value of three analyses). It was observed (Figs. 2 a and b) that the intensity and sharpness of the d(001) peak is maintained in the diffractograms of the TPS/NC film, which indicates the presence of nanostructured crystalline composites (Arellano-Cárdenas *et al.*, 2012). This is also a function of the amount of plasticizer added to the samples, since a lower proportion forms exfoliated structures and loses the crystallinity. This was reported by Tang *et al.*, 2005, who used 15 and 20% glycerol to form biofilms and obtained intercalated nanoclays. Wilhelm *et al.*, 2003, demonstrated using X-ray diffraction
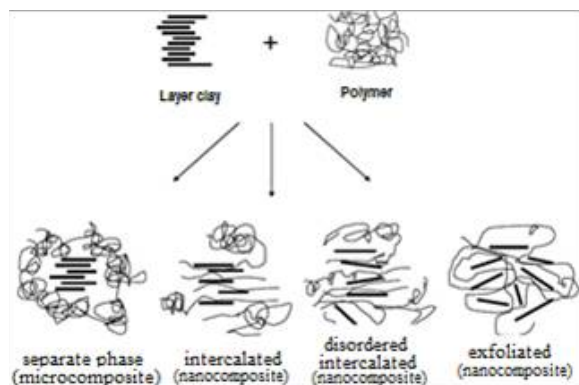
Fig. 3 Schematic depicting of the intercalation nanocomposites between polymer and sheets of clay (Ray and Bousmina, 2005).

on TPS/NC films that glycerol is intercalated in the interlaminar space of the clay, and the films made without glycerol showed completely exfoliated clay in the starch matrix; therefore, the corresponding peak did not appear in the XRD pattern. On the other hand, the same figures show a displacement of the peak to smaller 2θ angles, which implies an increase in the interlaminar distance compared to NC (1.24 nm). All the composite films showed an increase in the basal spacing of the layers, and the TPS/NC 85/15 film with 30% glycerol had the highest value, 1.82 nm (an increase of 32%) (Table 2). This may be due to the intercalation of starch and glycerol molecules in the interlaminar space of the clay to form interspersed starch/clay nanocomposites, as suggested by some authors (Santos *et al*., 2014; Cheviron *et al*., 2016; Zhang *et al*., 2007; Müller *et al*., 2012; Chen and Evans, 2005). Fig. 3 depicts the intercalation or exfoliation phenomenon that may occur between the polymers and clay as reported by Ray and Bousmina, 2005, and the phenomenon depends on the particular starch/clay proportions (Azeredo, 2009; Weiss *et al*., 2006).

Figs. 2 (c) and (d) show a large decrease in the intensity and sharpness of the first peak, d(001), in the three TPS/OC samples compared to OC, indicating the presence of compounds with low crystallinity that may have formed through a disordered intercalation process, as reported by Ray and Bousmina, 2005 (Fig. 3). The decrease in the peak intensity could be because during the preparation of OC, the clay was first intercalated with the CPC polymer, and, subsequently, in the films, starch and glycerol were interspersed in the free spaces, contributing to the exfoliation and loss of crystallinity. Hsin-Tzu and Chin-San, 2004, studied OC-CPC formulas in different proportions (0 to 12%) and observed with X-ray diffraction that the exfoliation phenomenon occurs at lower clay proportions. The same figures (Figs. 2 c and d) also show a displacement of the peak to lower 2θ angles, i.e., from a value of 4.12° for OC to a mean value of 3.5° for the TPS/OC films with three clay proportions (Table 2). This displacement implies an increase of 16% in the average basal distance from 2.14 to 2.55 nm, which is lower than the interlaminar increase in the TPS/NC film (32%) and may be due to a lower affinity between the hydrophobic OC and the hydrophilic starch and glycerol molecules (Santos *et al*., 2014; Müller *et al*., 2012).

3.4 Scanning electron microscopy (SEM) of the films

Fig. 4 shows the micrographs of a) TPS, b) TPS/NC, and c) TPS/OC films, the last two films were made with 90/10 starch/clay ratio with 30% glycerol. The homogeneous appearance of the TPS/NC film is due to the good dispersion of its components. On the other hand, the TPS/OC films seem heterogeneous, which may be explained by the lack of affinity between the hydrophilic starch and glycerol matrix with the modified, hydrophobic clay (Park *et al*., 2003; Zhang *et al*., 2007).
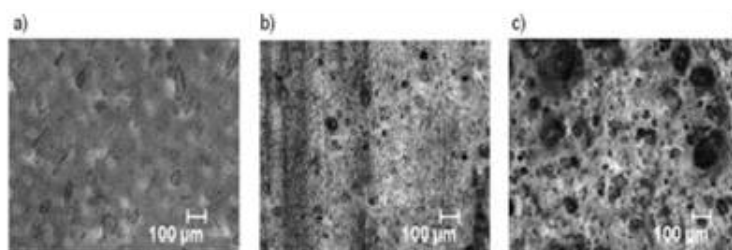

Fig. 4 SEM micrographs of a) TPS b)TPS/NC 90/10, 30% of glycerol, and b) TPS/OC 90/10, 30% of glycerol starch/clay composite films.

Table 3: Tensile strength (TS) and Young's Modulus (E) of TPS pure starch composite films with 25% and 30% glycerol content.

glycerol content (%)	TS (MPa)	E (GPa)
25	112.25±18.03	1.116±0.122
30	33.69±0.06	0.42±0.001

3.5 Mechanical properties of the films

The mechanical properties of the samples depend on the type of clay used in the formula and the amount of plasticizer. These also depend on the dispersion degree and the compatibility of the clay and plasticizer with the starch. Table 3 summarizes the tensile strength (TS) and Young's modulus (E) of the pure TPS films. As the glycerol content increases from 25 to 30%, the TS and E values have a significant decrease. It is known that a low E value indicates a higher elasticity; therefore, the addition of glycerol gives the films less strength and more elasticity because the glycerol molecules may facilitate the movement of the starch chains, increasing the flexibility (Tang *et al.*, 2005; Chang *et al.*, 2010; Koh *et al.*, 2008).

On the other hand, the mechanical properties of the films measured using the nanoindentation method were affected by the clay dispersion. Therefore, a statistical analysis was carried out on all the data obtained from the clays (NC and OC), the three combinations of starch/clay (95/5, 90/10, 85/15) and the two concentrations of glycerol (25 and 30%). The results obtained are shown in a main effect graphics.

Fig. 5 (I) shows the effect of the starch/clay ratio on the strength of the films. The TS increases as the clay (NC or OC) content increases, and the hardest structures are the 85/15 starch/clay ratio films. These results agree with other reports. Sothornvit *et al.*, 2009, proposed that the mechanical properties of biofilms such as hardness, may be attributed to the high rigidity of the structure and the affinity between the biopolymer and the particular type of clay. The same Fig. 5 (I) shows that increasing the glycerol content decreases the hardness of the films, as mentioned before.

The Young's modulus values were also affected by the clay dispersed in the polymer matrix, therefore, a statistical analysis was also performed on all the data. The results are shown in Fig. 5 (II). The significant effect of the starch/clay ratio on the elasticity is observed, and the films with the lowest elasticity are also the hardest, with a ratio of 85/15. This behavior is common in polymer materials reinforced with silicate fillers (Nguyen *et al.*, 2016; Romero-Bastida *et al.*, 2015). According to Muller *et al.*, 2012, the addition of clay to biofilms confers hardness due to the formation of intercalated structures. Park *et al.*, 2003, reported that a better clay dispersion results in better mechanical properties. The effect of glycerol on the elasticity of the films is also statistically significant, resulting in a higher elasticity at a concentration of 30% glycerol.

However, all the TPS/clay films had a lower elasticity than the pure TPS films. Nevertheless, it is possible to obtain starch films that show moderate mechanical properties by choosing the appropriate concentration of clay and glycerol.
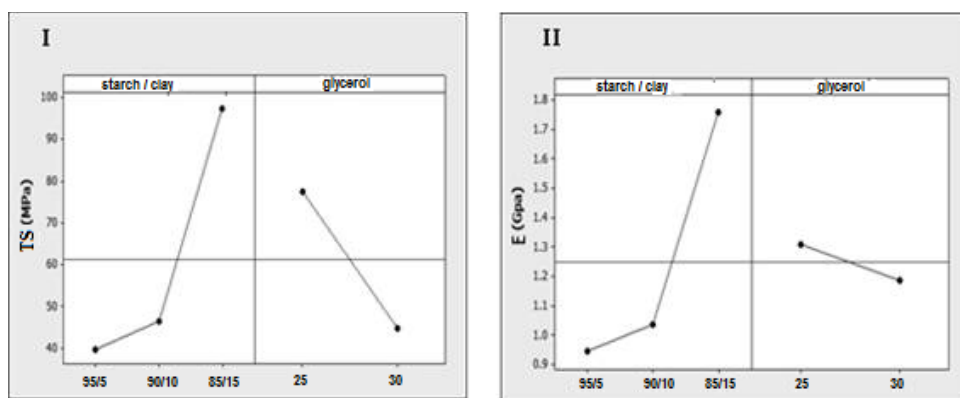

Fig. 5 Graphic of principal effects constructed with statistical analysis using all data obtained from clays (NC and OC) of: I) tensile strength (TS), II) Young's modulus (E) of the TPS/clay and glycerol (25% and 30%) composite films.
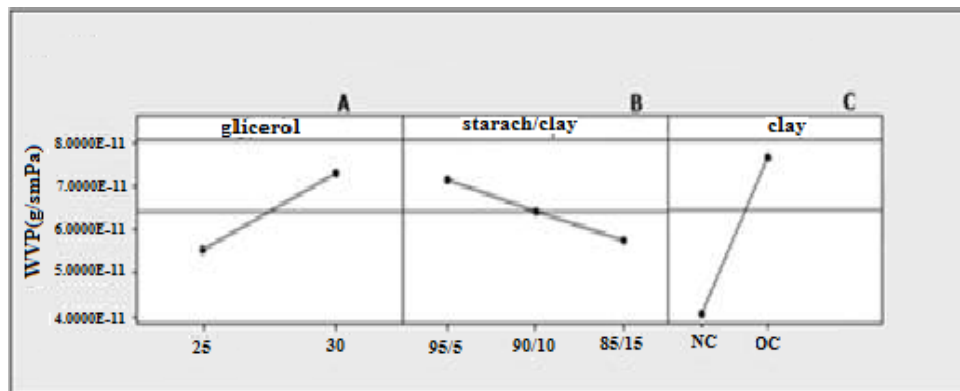
Fig. 6 Graphic of principal effects of water vapor permeability (WVP): A) as a function of glycerol content, B) as function of TPS/clay proportion, C) as a function of clay type.

3.6 Water vapor permeability (WVP) of the films

Fig. 6 presents a statistical analysis showing the independent effect of each variable on the WVP on the films made with two types of clay (NC and OC), three starch/clay ratios, and glycerol at 25 and 30%. The effect of glycerol is statistically significant on the WVP (Fig. 6 A), and the highest permeability was found on the films with 30% glycerol compared to 25%. This may be due to the formation of hydrogen bonds between the glycerol and starch molecules, which replace the interaction between the hydroxyl groups of the starch and silicate sheets in clay. Therefore, high glycerol content increases the hydrophilic character of the starch films. These results agree with the report by Tang *et al.*, 2005. Al-Hassan and Norziah, 2012, also mentioned that the hydrophilic character of the plasticizer increases the water vapor permeability, which in turn has a positive effect on the water vapor transfer velocity.

The WVP of films decreases when the proportion of clay (NC or OC) increases (Fig. 6 B), and this may be due to the higher number of silicate sheets dispersed in the matrix of the sample. However, the water vapor permeability also depends on the thickness of the film and the amount of plasticizer used in the formula, as shown in Table 4. It was observed that the permeability of the TPS/NC film (95/5 and 25% glycerol) was 4.11x10-11(g/smPa), which is higher than the reported by Ning *et al.*, 2010 (0.23x10-11 g/smPa), who used the same proportion in their TPS/NC films with 5% glycerol. The same fact occurs with the TPS/OC film, which had a higher permeability value than that
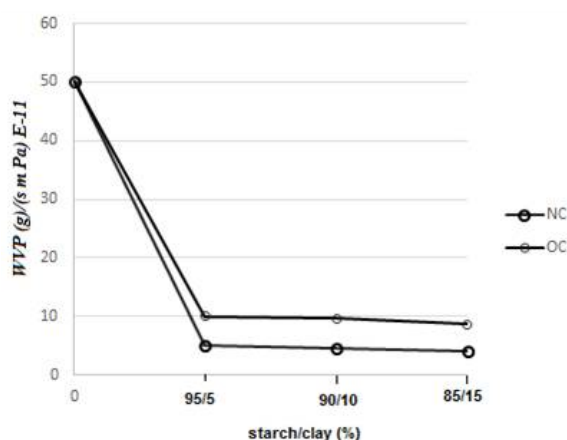

Fig. 7 Water vapor permeability (WVP) of TPS/NC and TPS/OC starch/clay composite films with 30% of glycerol. WVP of control TPS (pure starch) = 50×10^{-11} (g/smPa). Note: the experimental error for each point is 0.02 in average.

reported by Rhim *et al.*, 2009, for an organic clay.

On the other hand, it was also observed that WVP is a function of the particular type of clay (Fig. 6 C). The TPS/OC films showed higher WVP values compared to the TPS/NC films. This may be due to the lower crystallinity and heterogeneity in the former, as demonstrated by the X-ray diffraction and electronic microphotography results, because a lower dispersion of OC in the matrix decreases the tortuosity and favors water permeability. These results agree with Park *et al.*, 2003, who observed better barrier properties in films made from natural sodium clay (Cloisite Na^+) than in films made from Cloisite 30B, which is partially hydrophobic.

800

Table 4: Water vapor permeability (WVP) at 25 °C and RH (50 to 60%) of TPS/NC and TPS/OC 95/5 starch/clay composite films with 25% glycerol content.

Composition TPS/clay	WVP (g/smPa)	Thickness (mm)	Reference
TPS/ clay (95/5, 5\% glycerol)	0.23×10^{-11}	60	Ning *et al.*, 2010
PLA/NC	2.08×10^{-11}	80	
PLA/Cloisite 30B (OC) (Both 95/5)	1.7×10^{-11}	79	Rhim *et al.*, 2009
TPS/NC (95/5, 25% glycerol)	4.11 x 10-11	75	This work
TPS/OC (95/5, 25% glycerol)	6.76 x 10-11	83	This work

Fig. 7 shows the WVP of the TPS/NC and TPS/OC composite films compared to TPS pure starch using 30% glycerol. The same trend is observed with 25% glycerol. This figure shows that the WVP (average value $< 10 \times 10^{-11}$ g s^{-1} m^{-1} Pa^{-1}) of the films prepared with clay (NC or OC) is 80% lower than that of the films based on only starch (50×10^{-11} g s^{-1} m^{-1} Pa^{-1}). This decrease has been reported for starch/clay nanocomposites (Park *et al.*, 2003) and has been attributed to the dispersion of the silicate sheets in the matrix of the polymer. This obstructs the starch hydroxyl groups decreasing the transmission of water vapor through the matrix or from slowing water diffusion due to the generated tortuosity (Müller *et al.*, 2012; Ning *et al.*, 2010). The process of mass transfer depends on the affinity between the water and the polymeric matrix and on the resistance to the molecular movement of water within the matrix (Ning *et al.*, 2010).

Conclusions

Mechanical and barrier properties are improved when using clay materials as additives in starch-based films. The thickness of the resulting films depends on the type and proportion of the particular clay. The strength is greater when the concentration of the clay increases, and the elasticity is greater when the lowest proportion of clay is used and the glycerol content is increased. Films made with both types of clay, NC or OC, have decreased water vapor permeability by 80%, compared to films prepared with only starch.

Nomenclature

CEC	Cationic exchange capacity
E	Young's Modulus
NC	Natural clay
OC	Organoclay
TPS	Thermoplastic starch
TS	Tensile strength
WVPTR	Water vapor transmission rate
WVP	Water vapor permeability

References

Al-Hassan, A.A., Norziah, M.H. (2012). Starch gelatin edible films water vapor permeability and mechanical properties as affected by plasticizers. *Food Hydrocolloids 26*, 108-117.

Almazán-Sánchez, P.T., Solache-Ríos, M.J., Linares-Hernández, I., Martínez-Miranda, V. (2016). Adsorption-regeneration by heterogeneous fenton process using modified carbon and clay materials for removal of indigo blue. *Environmental Technology (United Kingdom) 37*, 1843-1856.

Arellano-Cárdenas, S., Gallardo-Velázquez, T., Poumian-Gamboa, G.V., Osorio-Revilla, G.,

López-Cortez, S., Rivera-Espinoza, Y. (2012). Sorption of naringin from aqueous solution by modified clay. *Clays and Clay Minerals 60*, 153-161.

Arellano-Cárdenas, S., López-Cortez, S., Cornejo-Mazón, M., Mares-Gutiérrez, J.C. (2013). Study of malachite green adsorption by organically modified clay using a batch method. *Applied Surface Science 280*, 74-78.

Avella, M., De Vlieger, J., Errico, E., Fischer, S., Vacca, P., Volpe, M. (2004). Biodegradable starch/clay nanocomposite films for food packaging applications. *Food Chemistry 93*, 467-474.

Averous, L., Boquillon, N. (2004). Biocomposites based on plasticized starch: thermal and mechanical behaviors. *Carbohydrate Polymers 56*, 111-122.

Azeredo, H. (2009). Nanocomposites for food packaging applications. *Food Research International 42*, 1240-1253.

Borges, J.A., Romani, V.P., Cortez-Vega, W.R., Martins, V.G. (2015). Influence of different starch sources and plasticizers on properties of biodegradable films. *International Food Research Journal 22*, 2346-2351.

Brindley, G., Brown, G. (1980). *Crystal Structures of Clay Minerals and their X-ray Identification*. Third edition. Mineralogical Society, London

Chang, P., Jian, R., Zheng, P., Yu, J., Ma, X. (2010). Preparation and properties of glycerol plasticized-starch (GPS)/cellulose nanoparticle (CN) composites. *Carbohydrate Polymers 79*, 301-305.

Chen, B., Evans, J. (2005). Thermoplastic starch-clay nanocomposites and their characteristics. *Carbohydrate Polymers 61*, 455-463.

Cheviron, P., Gouanvé, F., Espuche, E. (2016). Preparation, characterization and barrier properties of silver/montmorillonite/starch nanocomposite films. *Journal of Membrane Science 497*, 162-171.

Chung, Y.L., Ansari, S., Estevez, L., Hayrapetyan, S., Giannelis, E.G., Lai, H.M. (2010). Preparation and properties of biodegradable starch-clay nanocomposites. *Carbohydrate Polymers 79*, 391-396.

Cyras, V., Manfredi, L.B., Ton-That, M., Vázquez, A. (2008). Physical and mechanical properties of thermoplastic starch/montmorillonite nanocomposite films. *Carbohydrate Polymers 73*, 55-63.

Dean, K., Dieu, M., Petinakis, E., Yu, L. (2008). Key interactions in biodegradable termoplastic starch/poly(vinyl alcohol)/montmorillonite micro- and nanocomposites. *Composites Science and Technology 68*, 1453-1462.

Demirgöz, D.E. (2000). Chemical modification of starch based biodegradable polymeric blends: effects on water uptake, degradation behavior and mecanical properties. *Polymer Degradation and Stability 70*, 161-170.

Esmaeili, M., Pircheraghi, G., Bagheri, R. (2017). Optimizing the mechanical and physical properties of thermoplastic starch via tuning the molecular microstructure through co-plasticization by sorbitol and glycerol. *Polymer International 66*, 809-819.

Fialho e Moraes, A.R., Pola, C.C., Bilck, A.P., Yamashita, F., Tronto, J., Medeiros, E.A.A., Soares, N.D.F.F. (2017). Starch, cellulose acetate and polyester biodegradable sheets: effect of composition and processing conditions. *Materials Science and Engineering C 78*, 932-941.

Fisher, A.C. (2006). Critical review of analysis and interpretation of nanoindentation test data. *Surface and Coatings Technology 200*, 4153-4165.

Flores-Martínez, N.L., Valdez-Fragoso, A, Jiménez-Islas, H, Pérez-Pérez, M.C. (2017). Physical, barrier, mechanical and microstructural properties of Aloe vera-gelatin-glycerol edible films incorporated with *Pimenta dioica* L. Merrill essential oil. *Revista Mexicana de Ingeniería Química 16*, 109-119.

Gao, Y., Yangyong, D., Zhang, H., Enjie, D., Hanxue, H., Haizhou, D. (2014). Effects of organic modification of montmorillonite on the performance of starch-based nanocomposite films. *Applied Clay Science 99*, 201-206.

Hongguang, D., Chang, P.R., Geng, F., Yu, J., Ma, X. (2009). Preparation and properties of thermoplastic starch/montmorillonite nanocomposite using N-(2-Hydroxyethyl) formamide as a new additive. *Journal of Polymer Environment 17*, 225-232.

Hsin-Tzu, L., Chin-San, W. (2004). Synthesis and characterization of polyetylene-octene elastomer/clay/biodegradable starch nanocomposites. *Journal of Applied Polymer Science 97*, 397-404.

Huang, M., Yu, J., Ma, X. (2004). Studies on the properties of montmorillonite-reinforced thermoplastic starch composites. *Polymer 45*, 7017-7023.

Jiménez-Castañeda, M.E., Medina, D.I. Use of surfactant-modified zeolites and clays for the removal of heavy metals from water. *Water 9*, 1-12.

Khan, B., Bilal, Khan, Niazi, M., Samin, G., Jahan, Z. (2017). Thermoplastic starch: a possible biodegradable food packaging material-a review. *Journal of Food Process Engineering 40*, 1-17.

Koh, H., Park, J., Jeong, M., Hwang, H., Hong, Y., Ha, S., Nam, S. (2008). Preparation and gas permeation properties of biodegradable polymer/layered silicate nanocomposite membranes. *Desalination 233*, 201-209.

Lilichenko, N., Maksimov, R., Zicans, J., Merijs, M., Plume, E. (2008). A biodegradable polymer nanocomposite: mechanical and barrier properties. *Mechanics of Composite Materials 44*, 45-56.

López, S., Osorio, G., Gallardo, T., Arellano, S. (2008). Adsorption of vapor-phase VOCs (benzene and toluene) on modified clays and its relation with surface properties. *Canadian Journal of Chemistry 86*, 305-311.

Majdzadeh-Ardakani, K., Navarchian, A., Sadeghi, F. (2010). Optimization of mechanical properties of thermoplastic starch/clay nanocomposites. *Carbohydrate Polymers 79*, 547-554.

Muller, C.M.O., Laurindo, B.J., Yamashita, F. (2012). Composites of thermoplastic starch and nanoclays produced by extrusion and thermopressing. *Carbohydrate Polymers 89*, 504-510.

Müller, P., Kapin, E., Fekete, E. (2014). Effects of preparation methods on the structure and mechanical properties of wet conditioned starch/montmorillonite nanocomposite films. *Carbohydrate Polymers 113*, 569-576.

Nguyen, D.M., Vu, T.T., Grillet, A.C., Ha Thuc, H., Ha Thuc, C.N. (2016). Effect of organoclay on morphology and properties of linear low density polyethylene and Vietnamese cassava starch biobased blend. *Carbohydrate Polymers 136*, 163-170.

Ning, W., Xingxiang, Z., Na, H., Haihui, L. (2010). A Facile method for preparation of thermoplastic starch/urea modified montmorillonite nanocomposites. *Journal of Composite Materials 44*, 27-39.

Oliver, W., Pharr, G. (1992). An improved technique for determining hardness and elastic modulus using load and displacement sensing indentation experiments. *Journal of Materials Research 7-6*, 1564-1583.

Park, H., Lee, W., Park, C., Cho, W., Ha, C. (2003). Environmentally friendly polymer hybrids. Part I mechanical, thermal, and barrier properties of thermoplastic starch/clay nanocomposites. *Journal of Materials Science 38*, 909-915.

Ray, S.S., Bousmina, M. (2005). Biodegradable polymers and their layered silicate nanocomposites: in green the 21st century materials word. *Progress Material Science 50*, 962-1079.

Rhim, J., Hong, S., Ha, C.S. (2009). Tensile, water vapor barrier and antimicrobial properties of PLA/nanoclay composite films. *LWT-Food Science and Technology 42*, 612-617.

Romero-Bastida, C.A., Bello-Pérez, L.A., Velázquez, G., Álvarez-Ramírez, J. (2015). Effect of the addition order and amylose content on mechanical, barrier and structural properties of films made with starch and montmorillonite. *Carbohydrate Polymers 127*, 195-201.

Ruiz, G. (2006). Obtención y caracterización de un polímero biodegradable a partir del almidón de yuca. *Ingeniería y Ciencia 2*, 5-28.

Santos, R.A.L., Muller, C.O.M., Grossmann, M.V.E., Mali, S., Yamashita, F. (2014). Starch/poly (butylene adipate-co-terephthalate)/montmorillonite films produced by blow extrusion. *Quimica Nova 37*, 937-942.

Sothornvit, R., Krochta, J.M. (2001). Plasticizer effect on oxygen permeability of *β*-lactoglobulin films. *Journal of Food Engineering 48*, 6298-6302. Sothornvit, R., Jong-Whan, R., Seok-In, H. (2009). Effect of nano-clay type on the physical and antimicrobial properties of whey protein isolate/clay composite films. *Journal of Food Engineering 91*, 468-473.

Souza, A.C., Benze, R., Ferrão, E.S., Ditchfield, C., Coelho, A.C.V., Tadini, C.C. (2012). Cassava starch biodegradable films: Influence of glycerol and clay nanoparticles content on tensile and barrier properties and glass transition temperature. *LWT-Food Science and Technology 46*, 110-117.

Staroszczyk, H., Gottfried, K., Malinowska-Panczyk, E., Kolodziejska, I. (2017). Clay-filled starch films. Part I: effect of clay kind and glycerol concentration on functional properties of composites. *Starch/Starke 69*, 1-8.

Tang, X., Alavi, S., Herald, T. (2005). Effects of plasticizers on the structure and properties of starch-clay nanocomposite films. *Carbohydrate Polymers 74*, 552-558.

Villada, H.S., Acosta, H.A., Velasco, R.J. (2008). Research on thermoplastic starches, biodegradable products precursors. *Información Tecnológica 19*, 3-14.

Weiss, J., Takhistov, P., McClements, J. (2006). Functional materials in food nanotechnology. *Scientific Status Summary 71*, 107-116.

Wilhelm, H.M., Sierakowski, M.R., Souza, M.G.P., Wypych, F. (2003). Starch films reinforced with mineral clay. *Carbohydrate Polymers 52*, 101-110.

Wilpiszewska, K., Antosik, A.K., Spychaj, T. (2015). Novel hydrophilic carboxymethyl starch/montmorillonite. *Carbohydrate Polymers 128*, 82-89.

Yu, L., Dean, K., Li, L. (2006). Polymer blends and composites from renewable resources. *Progress in Polymer Science 31*, 576-602.

Yu, Z., Yin, J, Yan, S,. Xie, Y., Ma, J., Chen, X. (2007). Biodegradable poly(L-lactide)/poly(*ε*-caprolactone)-modified montmorillonite nanocomposites: preparation and characterization. *Polymer 48*, 6439-6447.

Zhang, Q., Yu, Z., Xie, X., Naito, K., Kagawua, Y. (2007). Preparation and crystalline morphology of biodegradable starch/clay nanocomposites. *Polymer 48*, 7193-7200.